Morphology of Multi-Walled Carbon Nanotubes Affected by the Thermal Stability of the Catalyst System

E. Dervishi,[†] Z. Li,[‡] A. R. Biris,[§] D. Lupu,[§] S. Trigwell,[||] and A. S. Biris*[,†,‡]

Applied Science Department, University of Arkansas at Little Rock, Arkansas, 72204, UALR Nanotechnology Center, Graduate Institute of Technology, University of Arkansas at Little Rock, Arkansas, 72204, National Institute for Research and Development of Isotopic and Molecular Technologies, P.O. Box 700, R-400293 Cluj-Napoca, Romania, and Electrostatic and Surface Physics Laboratory, Mail Code: ASRC-20, Kennedy Space Center, Florida 32899

Received September 19, 2006. Revised Manuscript Received November 9, 2006

High-quality multi-walled carbon nanotubes (MWCNTs) were efficiently synthesized on the $CaCO_3$ supported Fe−Co catalyst with catalytic chemical vapor deposition method using acetylene as carbon source. The relationship between the catalyst structure and the carbon nanotube growth was systematically studied by using multiple techniques including SEM, TEM, TGA, Raman spectroscopy, and XRD. It was found that the MWCNT product demonstrates two groups in the outer diameter distribution, which is associated with the partial decomposition of $CaCO_3$. This thermal decomposition was found to have as a result the coexistence of two catalytic systems throughout the entire synthesis process: Fe−Co/$CaCO_3$ and Fe−Co/CaO. It was also found that the smaller diameter nanotubes grow on the Fe−Co/CaO system, while Fe−Co/$CaCO_3$ produces larger diameter tubes.

1. Introduction

Carbon nanotubes (CNTs) are highly interesting materials because of their intricate chemical and physical properties and their wide range of possible applications. These range from physical applications such as composite fibers[1] or field effect transistors,[2] chemical applications such as hydrogen storage,[3] to possible biomedical applications.[4] Over the past decade, different production techniques have been developed, and the most commonly used approaches are arc discharge,[5,6] laser ablation,[7,8] and chemical vapor deposition.[9,10] Among these techniques, the catalytic chemical vapor deposition (CCVD) method attracts a lot of interest by making possible the large-scale and high-quality production of carbon nanotubes at a relatively low cost. Additionally, with the CCVD method, the growth of carbon nanotubes can be controlled by adjusting the reaction conditions and choosing proper catalysts.

In the CCVD method, carbon nanotubes are produced from the thermal decomposition of the carbon-containing molecules on desirable metal catalysts (commonly Fe, Co, and Ni). Many efforts have been put forth to optimize catalyst formulations and operating conditions.[11,12] The catalyst composition controlled by the preparation method affects the efficiency and selectivity of the catalytic reaction toward the synthesis of desired CNTs. Considering the strong correlation between the diameter of the nanotubes and the size of the catalytic metal particles, the high dispersity of the catalytically active metal ingredient on the support seems to be a critical point in the synthesis of carbon nanotubes by the CCVD method.[13]

In this contribution, we produced multi-walled carbon nanotubes (MWCNTs) on a calcium carbonate supported Fe−Co catalyst by using acetylene as a carbon source. The utilization of $CaCO_3$ as a support has many advantages over conventional supports like SiO_2 and Al_2O_3. The removal of the support and the catalysts of the catalytic system Fe−Co/$CaCO_3$ can be easily performed just by acid treatment, washing with distilled water, and filtration, which greatly reduces the purification cost. It was found that the partial decomposition of $CaCO_3$ supports under the reaction conditions results in two groups in the outer diameter distributions of MWCNTs. The effect of the catalyst's thermal behavior

* Corresponding author. Tel: (501) 683-7458. Fax: (501) 569-8020. E-mail: asbiris@ualr.edu.
[†] Applied Science Department, University of Arkansas at Little Rock.
[‡] Graduate Institute of Technology, University of Arkansas at Little Rock.
[§] National Institute for Research and Development of Isotopic and Molecular Technologies.
[||] Electrostatic and Surface Physics Laboratory.

(1) Kotov, N. A. *Nature (London)* **2006**, *442* (7100), 254.
(2) Javey, A.; Guo, J.; Farmer, D. B.; Wang, Q.; Wang, D.; Gordon, R. G.; Lundstrom, M.; Dai, H. *Nano Lett.* **2004**, *4* (3), 447.
(3) Nikitin, A.; Ogasawara, H.; Mann, D., Denecke, R.; Zhang, Z.; Dai, H.; Cho, K.; Nilsson, A. *Phys. Rev. Lett.* **2005**, *95* (22), 225507.
(4) Kam, N. W. S.; O'Connell, M.; Wisdom, J. A.; Dai, H. *PNAS* **2005**, *102*, 11600.
(5) Ebbesen, T. W.; Ajayan, P. M.; *Nature* **1992**, *358* (6383), 220.
(6) Ando, Y.; Zhao, X.; Inoue, S.; Suzuki, T.; Kadoya, T. *Diamond Relat. Mater.* **2005**, *14*, 729.
(7) Guo, T.; Nikolaev, P.; Thess, A.; Colbert, D. T.; Smalley, R. E. *Chem. Phys. Lett.* **1995**, *243* (1−2), 49.
(8) Maser, W. K.; Munoz, E.; Benito, A. M.; Martinez, M. T.; de la Fuente, G. F.; Maniette, Y.; Anglaret, E.; Sauvajol, J.-L. *Chem. Phys. Lett.* **1998**, *292*, 587.
(9) Endo, M.; Takeuchi, K.; Igarashi, S.; Kobori, K.; Shiraishi, M.; Kroto, H. W. *J. Phys. Chem. Solids* **1993**, *54* (12), 1841.
(10) Hernadi, K.; Konya, Z.; Siska, A.; Kiss, J.; Oszko, A.; Nagy, J. B.; Kiricsi, I. *Mater. Chem. Phys.* **2002**, *77*, 636.
(11) Kong, J. A.; Cassell, A. M.; Dai, H. *Chem. Phys. Lett.* **1998**, *292*, 567.
(12) Nikolaev, P.; Bronikowski, M. J.; Bradley, R. K.; Rohmund, F.; Colbert, D. T.; Smith, K. A.; Smalley, R. E. *Chem. Phys. Lett.* **1999**, *313*, 91.
(13) Dai, H.; Rinzler, A. G.; Nikolaev, P.; Thess, A.; Colbert, D. T.; Smalley, R. E. *Chem. Phys. Lett.* **1996**, *260*, 471.

10.1021/cm062237l CCC: $37.00
Published on Web 12/29/2006

on the characteristics of the nanotubes (diameter and crystallinity) was also investigated.

2. Experimental Design

The Fe−Co/$CaCO_3$ catalyst was prepared as previously explained by Couteau et al.[14] The stoichiometric composition of the catalyst was Fe/Co/$CaCO_3$ = 2.5:2.5:95 wt %. First, the weighted amount of metal salts $Fe(NO_3)_3 \cdot 9H_2O$ and $Co(CH_3COO)_2 \cdot 4H_2O$ were dissolved into distilled water with agitation, and $CaCO_3$ was added to the solution after the metal salts were completely dissolved. The pH value of the mixture solution was adjusted to about 7.5 by a dipping ammonia solution, to avoid the release of CO_2 occurring when carbonates contact acids.[15] Then, the water was evaporated with a steam bath under continuous agitation, and the catalyst was further dried at about 130 °C overnight.

Carbon nanotubes were synthesized on the Fe−Co/$CaCO_3$ catalyst with the CCVD approach using acetylene as a carbon source.[16] About 100 mg of the catalyst was uniformly spread into a thin layer on a graphite susceptor and placed in the center of a quartz tube with an inner diameter of 1 in., which was positioned horizontally inside a resistive tube furnace. Heating was applied after purging the system with nitrogen at 200 mL/min for 10 min, and acetylene was introduced at 3.3 mL/min for about 30 min when the temperature reached around 720 °C. These flow rates correspond to a linear velocity of the gas mixture inside the reactor of 40 cm/min. Therefore, it takes approximately 14 s for the acetylene/nitrogen mixture to travel from one side of the catalyst bed to the other (length of 9 cm). The as-produced CNTs were purified in one easy step using a diluted hydrochloric acid solution and sonication.

To understand the relationship between catalyst structure and carbon nanotube growth, the catalyst and CNTs were characterized by using scanning electron microscopy (SEM), transmission electron microscopy (TEM), thermogravimetric analysis (TGA), Raman scattering spectroscopy, and X-ray diffraction.

The morphologies of catalysts before and after 5 min of the growth reaction were monitored with a JEOL 6400F high-resolution scanning electron microscope. TEM pictures of the carbon nanotubes were obtained using a FEI Tecnai F30 transmission electron microscope. For this analysis, carbon nanotubes were dispersed in 2-propanol and ultrasonicated for 10 min. A few drops of the suspension were deposited on the TEM grid, then dried and evacuated before analysis.

Thermogravimetric analysis was used to study the thermal behavior of the catalyst system and to determine the overall purity of CNTs. Thermogravimetric analysis was performed under air flow of 150 mL/min using Mettler Toledo TGA/ SDTA 851e.

Raman scattering studies of the catalyst and CNTs were performed at room temperature using Horiba Jobin Yvon LabRam HR800 equipped with a charge-coupled detector, a spectrometer with a grating of 600 lines/mm and a He−Ne laser (633 nm) and Ar^+ (514 nm) as excitation sources. The laser beam intensity measured at the sample was kept at 5 mW. The microscope focused the incident beam to a spot size of <0.01 mm^2, and the backscattered light was collected 180° from the direction of incidence. Raman shifts were calibrated with a silicon wafer at a peak of 521 cm^{-1}.

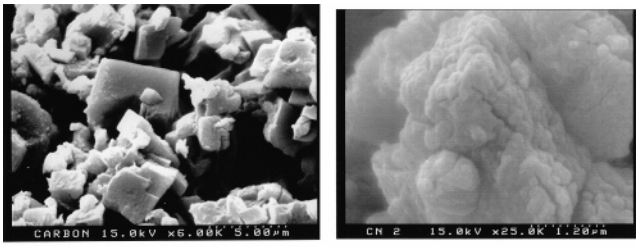

(a) (b)

Figure 1. SEM images of the catalyst Fe-Co/$CaCO_3$ (a) virgin and (b) after the thermal decomposition of $CaCO_3$ into CaO and CO_2. It is possible that there was a redistribution of the metal catalyst particles on the surface of the oxide support due to the thermal treatment.

An X-ray diffraction (XRD) technique was used for phase identification, quantitative phase analysis, and crystallite size estimation of catalyst. The X-ray power diffraction profiles of the catalyst system were recorded in the $\theta-2\theta$ mode on the Ultima III multipurpose diffraction system (Rigaku Corporation). The monochromatic Cu Kα radiation line and scintillation counter were used as excitation source and detector, respectively. The experiments were carried out in Bragg−Brentano geometry. Quantitative analysis was performed with whole pattern fitting and Rietveld refinement.

3. Results and Discussion

In Figure 1 , the SEM images of the Fe−Co/$CaCO_3$ catalyst are shown before and after 5 min of reaction. The virgin catalyst shows the presence of particles with flat surfaces having dimensions between 200 and 5000 nm. However, after 5 min of reaction, the catalyst was found to have a rougher surface because of the CO_2 release from the $CaCO_3$ support. The $CaCO_3$ support thermally decomposes into CaO at temperatures higher than 680 °C. These observations were consistent with the results of the following thermal, spectroscopic, and structural diffraction analysis. The BET surface areas were measured by krypton adsorption for both the virgin catalyst and the one collected after the thermal treatment and were found to be 6.2 and 7.3 m^2/g, respectively.

The TEM images and the diameter distribution histograms for over 200 carbon nanotubes are shown in Figure 2a,b. The MWCNTs were produced on the Fe−Co/$CaCO_3$ catalyst with acetylene as a carbon source at 720 °C, and the yield was found to be around 80%. The outer diameter distribution of these MWCNTs presents two groups, 8−35 and 40−60 nm. Approximately, 85% of the nanotubes has outer diameters from 8 to 35 nm, while the rest of them were in the range of 40−60 nm (Figure 2c). From the TEM analysis, it was observed that on the outer surface of the large diameter nanotubes, there is a layer of amorphous carbon (∼2 wt %), which was also observed in the TGA analysis. The presence of the amorphous carbon cannot be detected on the outer surface of the thinner nanotubes (8−35 nm).

Thermogravimetric analysis was performed to characterize the thermal behavior of the catalyst and the MWCNTs at air flow of 150 mL/min. Figure 3a shows the thermal behavior such as the weight loss profile and the decomposition rate of the Fe−Co/$CaCO_3$ catalyst, which was heated from room temperature to 850 °C at a rate of 5 °C/min. The TGA curve provides information about the thermal stability of the catalyst, and the first derivative of this curve

(14) Couteau, E.; Hernadi, K.; Seo, J. W.; Thien-Nga, L.; Miko, C.; Gaal, R.; Forro, L. *Chem. Phys. Lett.* **2003**, *378*, 9.
(15) Magrez, A.; Seo, J. W.; Mikó, C.; Hernádi, K.; Forró, L. *J. Phys. Chem. B* **2005**, *109* (20), 10087.
(16) Schmitt, T.; Biris, A. S.; Miller, D.; Biris, A. R.; Lupu, D.; Trigwell, S.; Rahman, Z. U. *Carbon* **2006**, *44* (*10*), 2032.

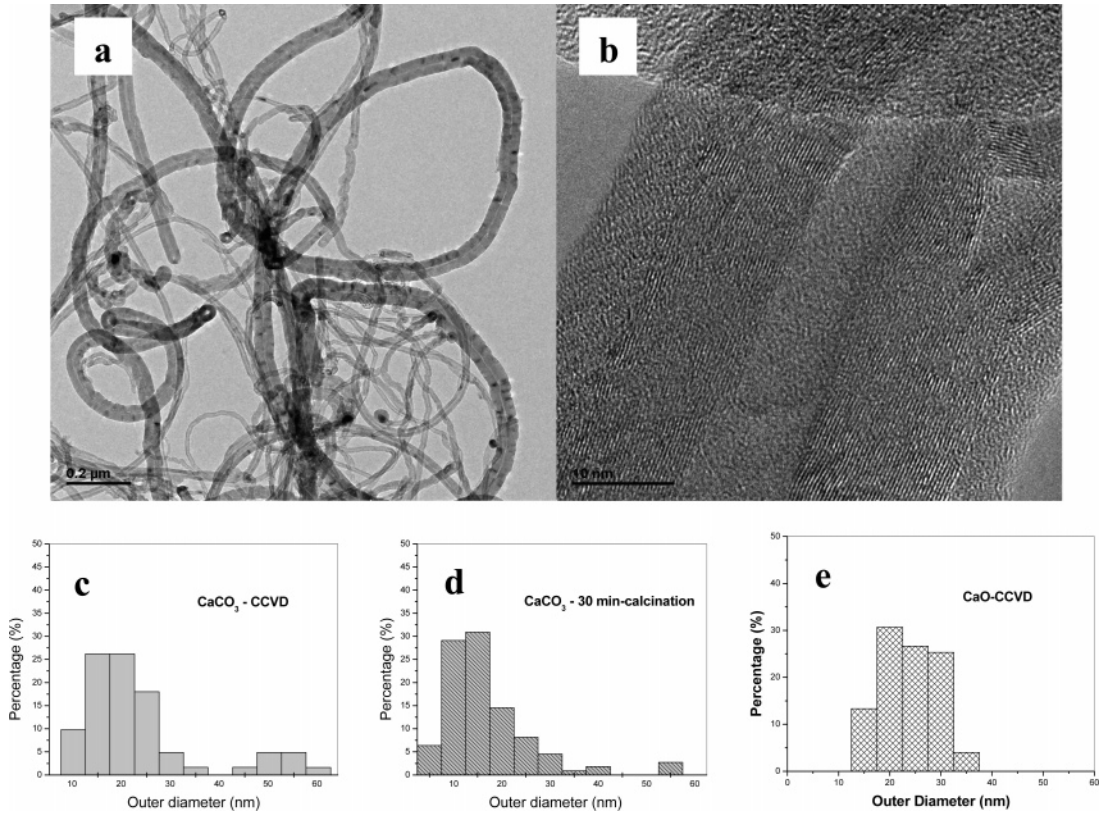

Figure 2. (a) TEM image of the MWCNTs obtained over a Fe-Co/$CaCO_3$ catalyst demonstrates carbon nanotubes with two different diameters. (b) TEM image of MWCNTs with large outer diameters. (c) Statistic diagram of MWCNTs with different diameters obtained from Fe-Co/$CaCO_3$ catalyst with acetylene as a carbon source. (d) Diameter histogram of the nanotubes grown on the Fe-Co/$CaCO_3$ catalyst calcinated at reaction temperatures for 30 min before acetylene was introduced. A shift of the nanotube diameters toward smaller values was observed due to the decomposition of $CaCO_3$ into CaO. (e) Outer diameter histogram of the carbon nanotubes grown on the CaO supported catalyst (Fe/Co/CaO = 4.3:4.3:91.4 wt %).

determines the maximum decomposition temperature of the sample. The initial mass of the Fe−Co/$CaCO_3$ sample was 3.826 mg, and the maximum rate of decomposition occurred at approximately 700 °C. The first weight loss peak (I) at around 130 °C corresponds to the evaporation of water that was present in the catalyst. The second set of peaks (II) in the weight loss profile of Fe−Co/$CaCO_3$ at 230 and 343 °C is due to the acetate and nitrate exhaustion from the catalyst. The last peak (III) around 700 °C is attributed to the release of CO_2 due to the thermal decomposition of the $CaCO_3$ support, which was found to occur between 680 and 850 °C. The weight loss profile showed that after the thermal decomposition, the mass of the catalyst decreased by approximately 45 wt %.

In a separate experiment, the weight loss profile of the Fe−Co/$CaCO_3$ catalyst was analyzed as a function of time using a similar temperature method as the growth process. The catalyst sample was heated from room temperature to 720 °C at a heating rate of 140 °C/min. This rate was chosen so that the time to reach the target temperature (720 °C) was about the same as the synthesis reaction that was performed to grow the nanotubes. It takes about 5 min to reach the reaction temperature during the synthesis. The reaction temperature was kept constant at 720 °C for 30 min just like in the synthesis of the carbon nanotubes. For the first 5 min, the weight loss was a result of water presence in the catalyst. After 5 min at around 720 °C, Fe−Co/$CaCO_3$ started to thermally decompose. The experimental results are shown in Figure 3b.

Thermogravimetric analysis is also a useful technique for characterizing the purity of carbon nanotubes. The weight loss profile in Figure 4 was obtained by heating the purified MWCNTs from room temperature to 850 °C at a rate of 5 °C/min. The first weight loss peak around 240 °C in the oxidation profile of MWCNTs is attributed to the oxidation of the amorphous carbon in the carbon nanotubes. For the nanotubes obtained after 30 min of the reaction, the amount of amorphous carbon was very small, less than 2% in total weight. The normalized TGA curve and its first derivative of the purified MWCNTs indicated a significant mass drop around 550 °C, which corresponds to the weight loss in the combustion of the MWCNTs. The quantitative analysis revealed that after the single-step purification, the purity of the MWCNT product was better than 95%.

To understand the structural change of the catalyst during the reaction under the presence of acetylene, we investigated the X-ray diffraction patterns of the virgin catalyst and the same catalyst collected after 5 min of the reaction. Figure 5 displays the powder diffraction profiles for the virgin Fe−Co/$CaCO_3$ catalyst and the one after 5 min of reaction. The crystalline structure and its composition can be easily identified by comparing the standard references and the whole pattern fitting with Rietveld refinement. The predominant phases present in the virgin sample are $CaCO_3$ (space group: $R\bar{3}c$, trigonal (167), a = 4.9896 Å, c = 17.0610 Å, and d = 3.04, 2.29, 2.10, 1.19, 1.88, 2.50, 3.86, and 1.60 Å), CoO_2, and Fe_2O_3. No mixed Fe−Co−Ca oxide phase was found, which indicates the absence of a reaction between

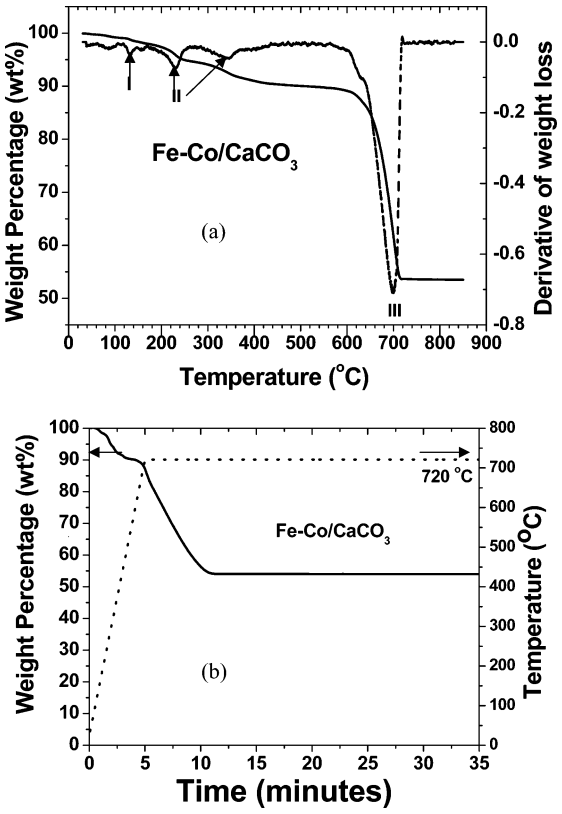

Figure 3. (a) Weight loss profile and burnoff rate of the Fe-Co/$CaCO_3$ catalyst. The peaks marked with arrows are due to the evaporation of water (I) and the acetate and nitrate exhaustion (II) and thermal decomposition of the $CaCO_3$ support (III), respectively. (b) Weight loss profile and temperature curve of Fe-Co/$CaCO_3$ vs time.

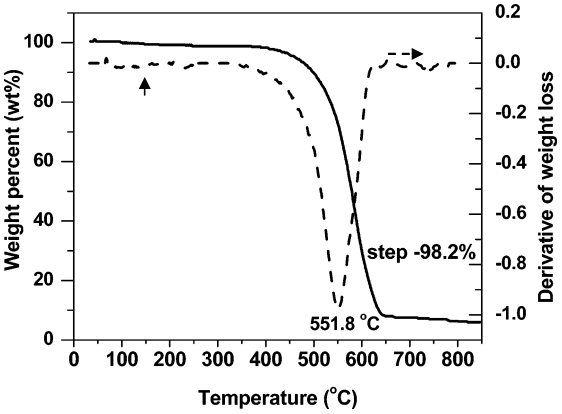

Figure 4. Weight loss profile and oxidation rate of MWCNTs obtained from Fe-Co/$CaCO_3$ catalyst. The arrow indicates the combustion of amorphous carbon.

Fe, Co, and $CaCO_3$ precursor salts, or the Fe and Co species might exist in a highly amorphous form. However, the XRD profile of the thermally treated catalyst shows additional peaks that are attributed to the most intense inflections of $Ca_2Fe_2O_5$ (space group: *Pnma* (62), $a = 5.4242$ Å, $b = 14.754$ Å, $c = 5.5983$ Å, and $d = 7.38, 3.69, 2.68, 1.84, 1.95, 2.80, 2.71$, and 20.8 Å) and CoO (space group: $Fm\bar{3}m$, cubic (225), $a = 4.2500$ Å, and $d = 2.13, 2.46, 1.51, 0.95, 1.28, 1.23, 0.98$, and 1.07 Å). The significant increase in the intensities of $Ca(OH)_2$ diffraction peaks is due to the thermal decomposition of $CaCO_3$ into CaO (space group: *Fm*3*m* (225), $a = 4.8106$ Å, and $d = 2.41, 1.70, 2.78, 1.45, 1.39, 1.08, 0.8$, and 0.98 Å) during the synthesis reaction.

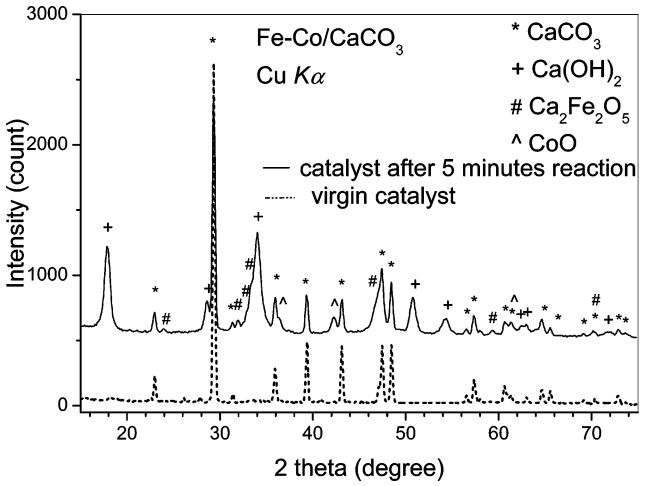

Figure 5. X-ray powder diffraction patterns for the virgin Fe-Co/$CaCO_3$ catalyst and that after 5 min of reaction.

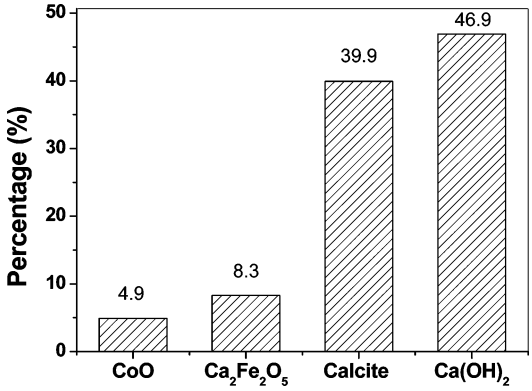

Figure 6. Rietveld analysis of the Fe-Co/$CaCO_3$ catalyst composition after 5 min into the reaction.

Table 1. Crystallite Size of Catalyst That Was Removed from Reactor after 5 Min into Reaction

phase	$CaCO_3$	CoO	$Ca(OH)_2$	$Ca_2Fe_2O_5$
crystallite size (nm)	81.3	19.5	13.5	34.6

CaO can absorb water easily in air and convert into $Ca(OH)_2$ since the sample was exposed to air during the structural and spectroscopic analysis. This explains the presence of strong diffraction patterns corresponding to the $Ca(OH)_2$ phase. The coexistence of $CaCO_3$ and CaO (or $Ca(OH)_2$) in the catalyst after 5 min of the reaction suggests that the decomposition of the $CaCO_3$ support in our reaction is not complete after the first few minutes. The crystal percentages of the compositions in the catalyst after 5 min of the reaction are $CaCO_3$ (39.9 wt %), $Ca(OH)_2$ (46.9 wt %), CoO (4.9 wt %), and $Ca_2Fe_2O_5$ (8.3 wt %), as shown in Figure 6. The weak diffraction peaks from the spinel Fe_2CoO_4 are also observed, which is believed to be the precursor of the active species, FeCo alloy, for the multi-walled carbon nanotube growth, as reported by Magrez et al.[15] The crystalline sizes estimated from the diffraction peak widths (using the Scherrer equation) are 81.3 nm ($CaCO_3$), 13.5 nm ($Ca(OH)_2$), and 19.5 nm (CoO). This explains the variation in diameter of the nanotubes, as seen in Table 1. The Rietveld structural data presented in Figure 6 agree nicely with the thermal decomposition behavior of the catalyst (Figure 3).

The TGA results revealed that about 85% of $CaCO_3$ decomposed during the reaction process. Additionally, about

80% of crystalline $Ca(OH)_2$ formed from CaO while exposed to air (H_2O) was discovered in Rietveld refinement analysis. Combining the TGA and XRD results, one can conclude that during the reaction, about 85% of $CaCO_3$ decomposed and converted into small sized crystalline CaO. The statistic analysis of TEM images of the MWCNT production revealed the two different outer diameter distributions, 85% of small diameter tubes and 15% of large diameter tubes. This might suggest that these two diameter distribution groups are associated with the decomposition of $CaCO_3$ during the reaction and that the smaller diameter tubes might grow on the small catalyst particle of CaO. At a temperature of 700 °C, $CaCO_3$ would be expected to decompose within 20 min; however, under our experimental conditions, it is possible that the decomposition was not complete,[8] leading to the coexistence of two catalyst systems (i.e., Fe−Co/$CaCO_3$ and Fe−Co/CaO). As compared with the $CaCO_3$ support, the newly generated CaO support presents a rougher surface (as seen in the SEM), which is expected to influence the distribution of catalyst particles on the support. Acetylene molecules decompose and begin to rearrange (nucleate) until a given configuration, and carbon surface concentrations are reached, which favor the formation of the nanotube. We propose calling this configuration the embryo. When this embryo (nucleation) is formed, the subsequent incorporation of carbon and CNT formation would proceed at a fast rate, perhaps controlled only by mass transfer.[17] As a result, one can expect that the nanotubes grown on Fe−Co/CaO have smaller diameters than those on Fe−Co/$CaCO_3$. This would explain the two domains of the outer diameter of the carbon nanotubes.

To confirm the hypothesis regarding the coexistence of the two catalyst systems, in a separate experiment, the Fe−Co/$CaCO_3$ catalyst was first thermally decomposed for 30 min at the reaction temperature (720 °C) before acetylene was introduced into the reactor. Since $CaCO_3$ is expected to decompose, the nanotubes grown in this situation should have mostly grown on the CaO supported catalyst. The histogram of the outer diameter values of these nanotubes is presented in Figure 2d. It can be observed that most of the nanotubes have outer diameters in the range of 5−35 nm with the maximum at around 18 nm. A few nanotubes with outer diameters of around 55 nm can still be observed, probably formed on the remaining (undecomposed) $CaCO_3$ supported catalyst. This experiment confirms the supposition that the catalyst on the newly formed CaO support generates thinner nanotubes. To find independent proof for this phenomenon, the Fe−Co catalyst was directly dispersed onto the CaO surface by dissolving the corresponding salts into ethanol solution. Considering about 45% mass loss of the $CaCO_3$ support, which translated the Fe and Co species to higher loading on the newly generated CaO support, the new composition was calculated to be Fe/Co/CaO = 4.3:4.3:91.4 wt %. This new catalyst was tested under the same reaction conditions as stated previously. The nanotubes grown on this catalyst have a more homogeneous outer diameter distribution as shown in Figure 2e. It clearly demonstrates that the thermal decomposition of $CaCO_3$ into CaO during the reaction leads to the growth of nanotubes with smaller diameters.

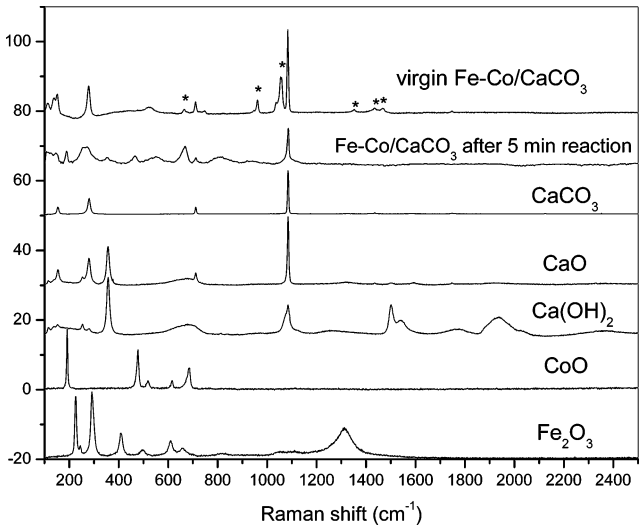

Figure 7. Raman scattering spectra from the Fe-Co/$CaCO_3$ catalysts and standard references. The stars mark the possible scatterings from the spinel-like Fe_2CoO_4.

The previous findings are also in agreement with the results provided by Raman spectroscopy. The Raman scattering from the virgin and thermally treated catalyst is shown in Figure 7 along with standard references. Since the total metal loading of the catalyst is only 5 wt %, the major Raman peaks correspond to the $CaCO_3$ support. The Raman scattering spectrum from $CaCO_3$ powder shows five peaks, one assigned to A_{1g} mode (1083 cm^{-1}) and four assigned to E_g modes (156, 282, 710, and 1432 cm^{-1}), in agreement with the previous papers.[18,19] The defect induced Raman peaks in CaO ranging from 150 to 600 cm^{-1} correspond to lattice vibrational bands of F and F^+ centers.[20] The sharp and intense peak at 1048 cm^{-1} corresponds to the localized vibrational mode of the H^{2-} ion in CaO. The rest of the weak Raman peaks (523, 746, 961, 1057, 1351, 1422, 1467, and 2940 cm^{-1}) might be given by the spinel-like $Ca_2Fe_2O_5$ and/or Fe_2CoO_4 since it was found in the previous XRD profile. The Raman spectroscopy results are in good agreement with the structural data presented in Figure 5. Both the spectroscopic and the structural analysis data indicate the thermal instability and the structural and morphologic changes of the catalytic system. Ultimately, the coexistence of the two catalysts will influence the variation in the nanotube properties.

The Raman scattering spectra from the MWCNTs grown on Fe−Co/$CaCO_3$ shown in Figure 8 were collected with two different laser excitation energies (633 and 514 nm). The larger nanotube diameters and the wider diameter distributions inherently present in the MWCNTs make it unlikely to be able to observe the nanoscale phenomena found in single-walled carbon nanotubes. The characteristic bands for MWCNTs are the D band, G band, and 2D band. The D band is present between 1305 and 1330 cm^{-1} and is

(17) Resasco, D. E.; Herrera, J. E.; Balzano, L. *J. Nanosci. Nanotechnol.* **2004**, *4*, 1.
(18) Liu, L. G.; Mernagh, T. P. *Am. Mineral.* **1990**, *75*, 801.
(19) Williems, Q.; Collerson, B.; Knittle, E. *Am. Mineral.* **1992**, *77*, 1158.
(20) Ke, S. C. *Phys. Rev. B* **2000**, *62* (7), 4194.

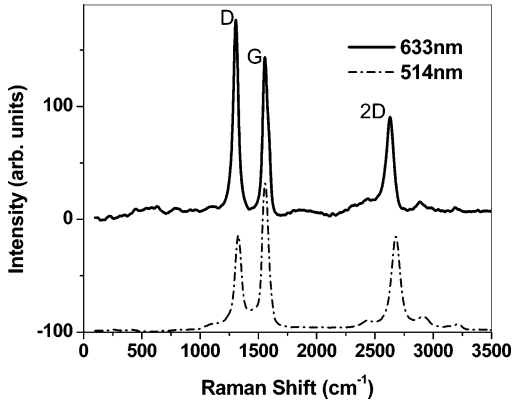

Figure 8. Raman scattering spectra of the MWCNTs produced on the Fe-Co/$CaCO_3$ catalyst with acetylene as a carbon source.

associated with defects and impurities in the carbon nanotubes. Furthermore, the frequency of the D band shifts upward as the laser excitation energy increases. Another characteristic band is the G band, which is present between 1500 and 1605 cm^{-1}, and it corresponds to the stretching mode of the carbon−carbon bond in the graphite plane. The G band position is relatively constant for the MWCNT material excited at different energies. The relative intensity of the D and G bands (I_D/I_G) decreases with increasing excitation energies. These observations are in agreement with the observations of Antunes et al.[21] The last important mode observed in the Raman spectrum of CNTs is the 2D band. This mode is a second-order harmonic of the D band, which is often present between 2450 and 2650 cm^{-1}. The 2D band is also highly dispersive and is usually associated with the degree of crystallinity of the carbon nanotubes. The presence of the G band and the dispersive behavior of the D band, together with fairly low value of half-height peak width (<40 cm^{-1}), indicate a high degree of graphitization of the MWCNTs grown on the Fe−Co/$CaCO_3$ catalyst. The relative intensity between the G and the D bands (I_D/I_G) was found to be 0.81 for the 633 nm laser and 1.52 for the 514 nm laser, respectively. Also, the ratios between the 2D and the G band intensities were found to be 0.63 for the 633 nm laser and 0.65 for the 514 nm excitation. These values indicate an inter-planar distance of 0.342 nm between the graphite layers, as shown by Yoshida et al.[22]

4. Conclusion

As previously shown,[14,16] this study also found that the $CaCO_3$ supported Fe−Co catalyst is very effective for the multi-walled carbon nanotube synthesis with the CCVD method using acetylene as a carbon source. The decomposition temperature of $CaCO_3$ into CaO and CO_2 is very close to the MWCNT growth temperature. This leads to the coexistence of two catalytic systems, Fe−Co/$CaCO_3$ and Fe−Co/CaO, throughout the entire synthesis period of MWCNTs. The difference in the specific surface areas between CaO and $CaCO_3$ results in the two different sizes of the metal clusters; as a consequence, the MWCNT product demonstrates two groups in the outer diameter distribution. On the basis of TGA, Raman scattering, and XRD analysis, we found that the smaller diameter nanotubes grow on the Fe−Co/CaO system while Fe−Co/$CaCO_3$ produces the large diameter tubes. High-purity MWCNTs can be achieved by a single-step acid washing, which makes the Fe−Co/$CaCO_3$ catalyst a very promising industrial product to produce high-quality MWCNT on a large scale and at a low cost.

Acknowledgment. This work was supported by the U.S. Department of Energy. We are also grateful to the XRD technical assistance from Dr. Akhilesh Tripathi (Rigaku Co.)

CM062237L

(21) Antunes, E. F.; Lobo, A. O.; Corat, E. J.; Trava-Airoldi, V. J.; Martin, A. A.; Veríssimo, C. *Carbon* **2006**, *44*, 2202.

(22) Yoshida, A.; Kaburagi, Y.; Hishiyama, Y. *Carbon* **2006**, *44*, 2330.